33RD CONGRESS
OF THE INTERNATIONAL COUNCIL
OF THE AERONAUTICAL SCIENCES
STOCKHOLM, SWEDEN, 4-9 SEPTEMBER, 2022

ICAS 2022 SWEDEN

CAD DEFORMATION FOR THE CONSIDERATION OF AEROELASTIC EFFECTS

Patrick Wegener[1], Stefan Keye[2]

[1] German Aerospace Center (DLR), Lilienthalplatz 7, 38108 Braunschweig
[2] German Aerospace Center (DLR), Lilienthalplatz 7, 38108 Braunschweig

Abstract

Wings of real aircraft are structures that deform elastically due to a variety of flight and ground loading conditions. In order to perform CFD simulations for the different flight conditions, the corresponding elastic wing deformations have to be considered. The method of mesh deformation used for this purpose requires transformation vectors from the unloaded to the deformed geometry as input. Since these are not always available from governing disciplines such as structural mechanics or wind tunnel experiments for a sufficient number of surface points, the vectors are usually determined from the available data by additional software tools [1]. In this paper, an approach to compute these transformations directly in CAD is described. The challenge in this case is to limit the deformation of the complex swept and twisted wing geometry to the elastic effects present in structural mechanics in order to avoid modifications of, for example, the wing surface, the wing planform or the airfoil thickness distribution. The method was applied to the NASA/Boeing Common Research Model (CRM) in wing/body configuration in order to provide aeroelastically deformed CAD geometries for the 7th AIAA Drag Prediction Workshop. Wing deformation input data for this application was obtained from the Trans National Access (TNA) test campaign at the European Transonic Wind Tunnel in Cologne, carried out during the European research project ESWIRP (European Strategic Wind tunnels Improved Research Potential) [2].

Keywords: CAD, Deformation, Aeroelasticity, Wind tunnel

1. Introduction

In the aerodynamic simulation of real objects, elastic deformation occurs depending on the load condition, which is of varying degree depending on the material and shape. Particularly in the case of wings of current commercial aircraft, this occurs not only in full scale but also in wind tunnel models due to their slender shape. A distinction is made between the, unloaded geometry state, the "jig shape", and the "flight shape", whose elastic deformation depends on the load. In order to be able to aerodynamically calculate different flight states with sufficient accuracy, the associated wing deformations must be considered. A common approach is shown in Figure 1: Starting from an initial CAD model, computational mesh and a CFD solution, a deformation is determined based on external influences such as wind tunnel results. From this, the deformation is described in the form of translation vectors, which are used to deform the computational mesh.

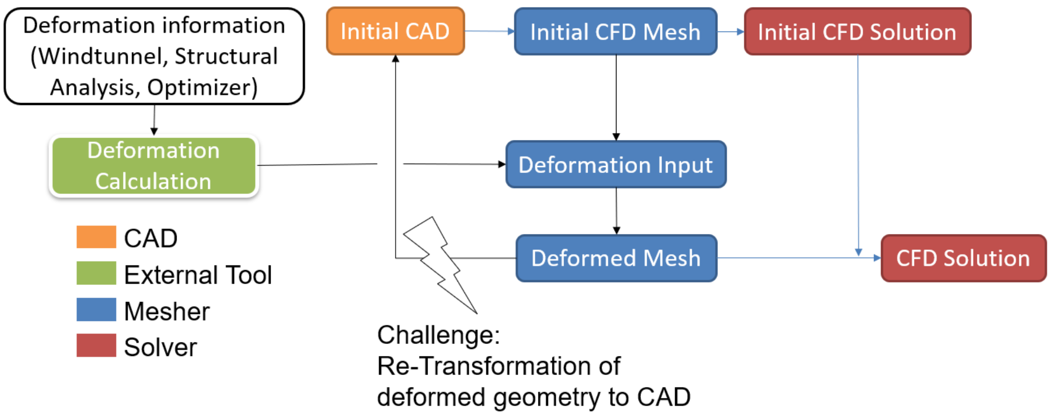

Figure 1: Simulation schema

An advantage is the reduction of computation time by reusing existing solutions. A disadvantage is the transfer of the results to spatial geometry for subsequent processes, since this requires a transfer of the deformed mesh to the geometric surfaces. An alternative approach is to deform the geometry directly in the CAD system (Figure 2): This allows a simulation of the new geometry via a regeneration of the CFD mesh (b).

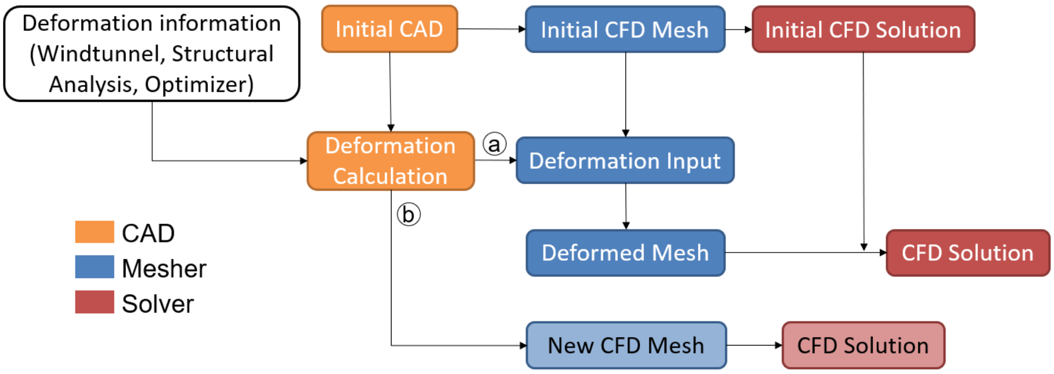

Figure 2 - Alternative approach for simulation

Since this method is more robust against larger geometric changes compared to mesh deformation, undeformed geometries such as pylon and engine can be considered on the deformed wing via subsequent CAD operations. If subsequently the translation vectors are computed in CAD, the previous way (a) is also possible, with the advantage of acceleration and simplification by eliminating the external process for deformation computation. The approach of deforming the surface data based on wind tunnel information has already been described [1].
In contrast to this approach, in the present work these deformations are performed completely within the CAD system. The challenge here is to limit the deformation on the complex swept and twisted wing geometry to the elastic effects that are plausible in terms of structural mechanics in order to avoid unintentional changes in, for example, the wing area, the wing planform or the airfoil thickness distribution.

2. Wind tunnel test

Since 2001, the drag of transonic aircraft configurations, especially in the range of off-design conditions, has been scientifically investigated by experimental analysis and numerical simulation in the form of the "Drag Prediction Workshop" series [3]. As part of the European research project ESWIRP (European Strategic Wind tunnels Improved Research Potential) [2], aeroelastic wing bending and twisting deformations of the NASA CRM model [4] were recorded during the Trans National Access (TNA) test campaign at the European Transonic Wind Tunnel in Cologne.

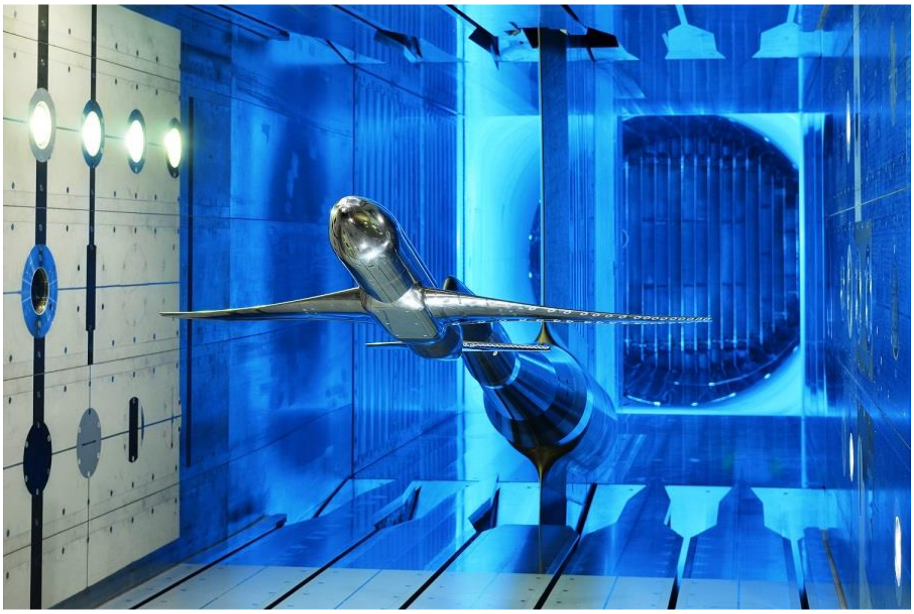

Figure 3 - CRM wing/body model in European Transonic Wind Tunnel [5] [Photo: © ETW]

As shown in Figure 3 on the left wing lower side, coordinates were determined at 11 wing sections in the spanwise direction at defined distances from the leading and trailing edges to determine the vertical displacement of their midpoint and the difference in twist compared to the unloaded case. Based on these data, the aeroelastic deformation of the wind tunnel model is to be considered in the accompanying CFD simulations. Deformation data for the flow conditions defined for the CRM test cases and the required angle of attack range were available from runs no. 182 and no. 237 (Table 1).

Run No.	Ma_∞	Re / [10^6]	$p_{tot.}$ / [kPa]	$T_{tot.}$ / [K]	q/E
182	0.85	5.0	191.0	264.0	0.3260
237	0.85	30.0	303.0	101.8	0.4936

Table 1 - Flow conditions of selected reference test runs from ETW test campaign

As the measured angles of attack from the acquired data points slightly differ from the predetermined angles, an interpolation of measured deformations to the exact angle of attack values from the test case definitions has been performed prior to applying the CAD deformation process (Figure 4).

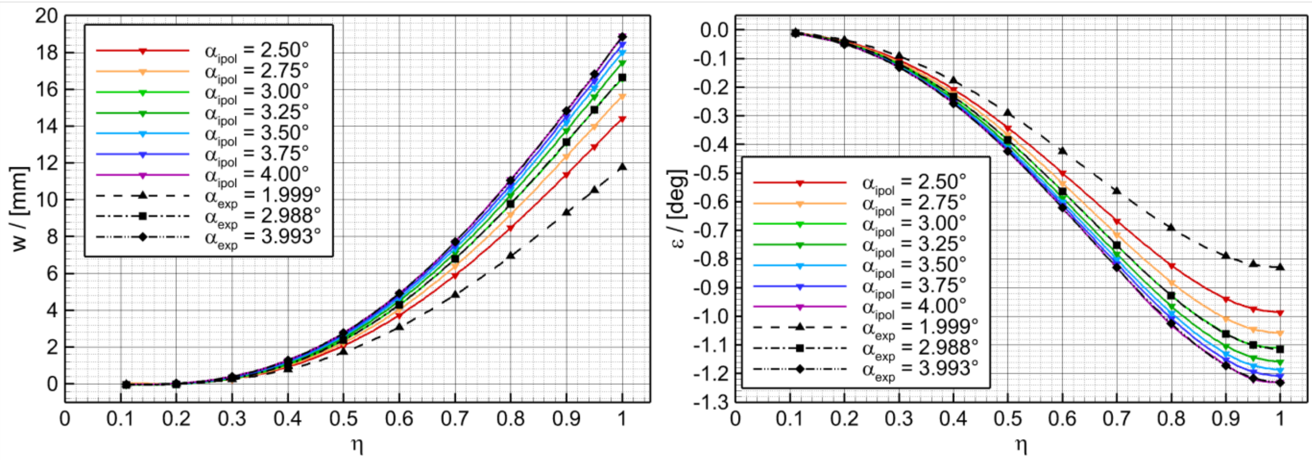

Figure 4 - Measured and interpolated wing bending and twist deflections: ETW test run no. 182

3. CAD transformation

The CAD system "CATIA" from Dassault Systèmes is used in the academic context for modeling CFD geometries [6]. In the present work, the geometry of the CRM model provided by NASA [7] forms the reference. To determine the elastic deformation, the function "Wrap surface" from the workbench "Generative Shape Optimizer" is used: This allows the deformation of a geometry based on the differences between a reference and a target surface. In this case, the wing geometry of the unloaded windtunnel model represents the input geometry of this deformation. In the applied case, the geometry is processed with the "Normal Transformation" option.

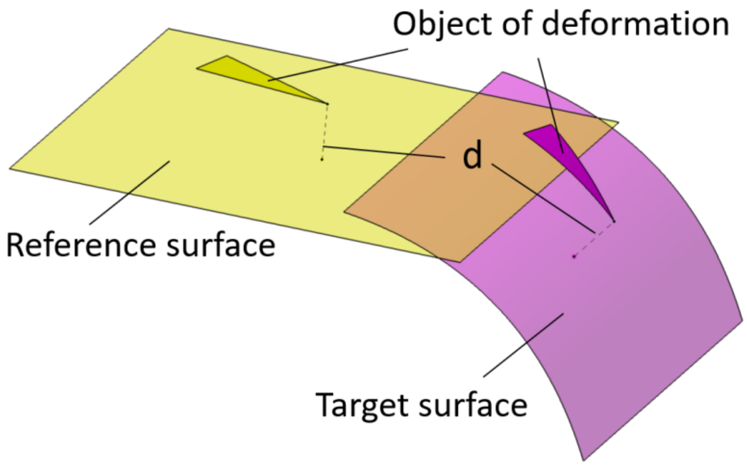

Figure 5 - Schematic representation of the normal transformation

The mathematical basis of this function is shown schematically in Figure 5: The reference surface is colored in yellow, the target surface in magenta. For each point - in the example the tip of the triangle of the object to be deformed - a projection in normal direction onto the reference surface is performed. From this, the U/V coordinate of the projection and the projection distance are calculated. The corresponding U/V coordinate is then determined on the target surface. Together with the distance d, this results in the new coordinate, and in the sum of all points, the deformed surface.
One recognizes in this respect the challenge of the surface quality between reference and target surface: The curvature as well as the distance to the deformed object influences the quality of the result. Furthermore, reference and target surface should be created in a mathematically analogous way to ensure a correct assignment of the UV coordinates.

Modelling the transformation surfaces

To determine the reference surface, the layout of the measuring points from the experiment was reconstructed (Figure 6): On the lower surface, the curves of 5 and 95% chord were determined. These were intersected at all 11 spanwise positions, and their center point determined. The connection between front and rear point gives the local torsion for each spanwise position.

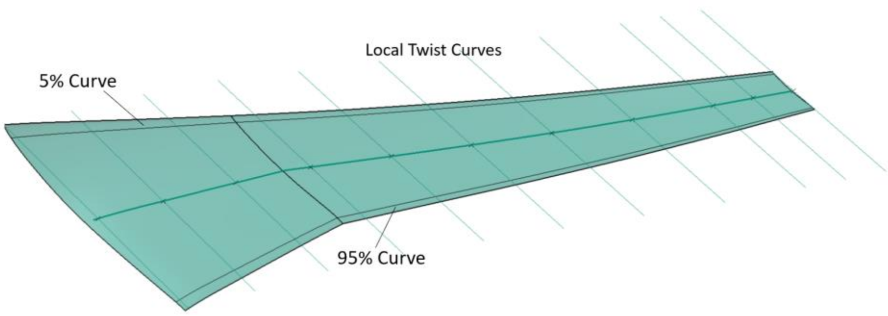

Figure 6 - Determination of the reference surface

Wing bending

Based on the wind tunnel test, the vertical displacements for the spanwise positions are given. To explain the transfer into the three-dimensional deformed geometry, the setup is shown on a two-dimensional example:

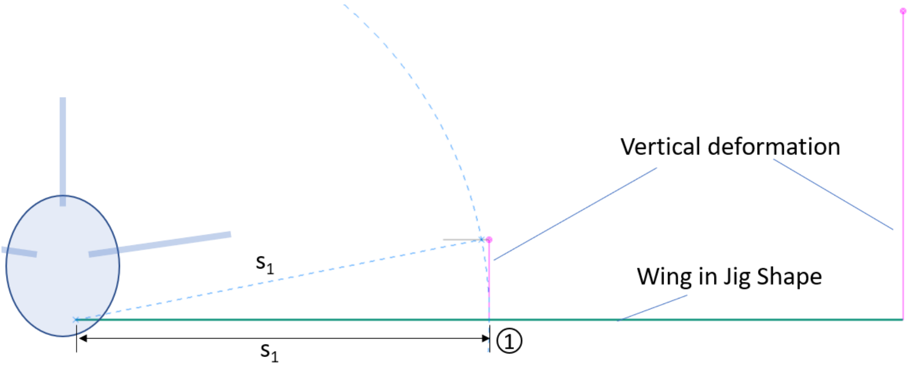

Figure 7 - Vertical deformation, segment 1

Figure 7 shows the schematic representation of the aircraft viewed from the rear. The green curve represents the wing in jig shape, with 0° dihedral for simplicity. The 11 intersections in spanwise direction were determined on this curve. For simplification, only 3 points are shown here. To calculate the deformation at position 1, a circle is drawn starting from the wing root with the radius of the distance between point 0 and 1 (s1) to the next segment. The horizontal projection of the first vertical displacement gives the first point of the deformed wing.

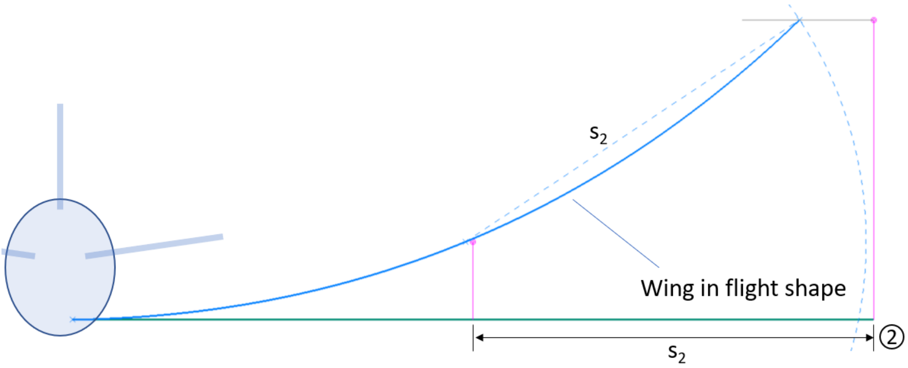

Figure 8 - Vertical deformation, segment 2

In Segment 2, this first point forms the center of the next circle with the radius of the next spanwise segment distance s2 (Figure 8). Again, the projection of the vertical displacement forms a point of the deformed wing. The connection of all points of the deformed wing by a spline curve forms its new center curve.

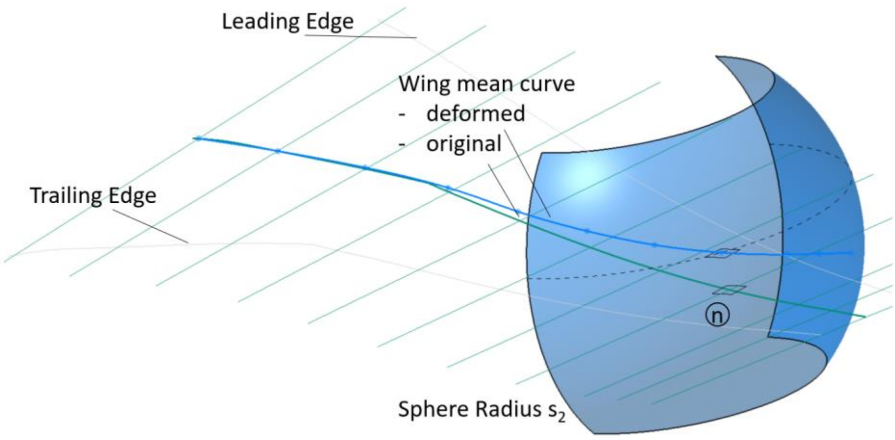

Figure 9 - 3D curve

Figure 9 shows the transfer of the scheme to the spatial case: The circle becomes a spherical surface, the vertical distance is generated by an offset plane intersecting the spherical segment. The new coordinate is obtained by projecting the n-th reference point onto the intersection line.

Twist transformations

Figure 6 shows the local twist curves. Following the previous transformation, 11 curves are built up by the determined points of the local displacement, in which the curves are each rotated by the angle of the elastic deformation. The axis of rotation is the normal to the plane of symmetry. The reference and target surfaces are each generated by the 11 curves determined in this way. Thus, the transformation of the complete wing including the wing tip can be performed:

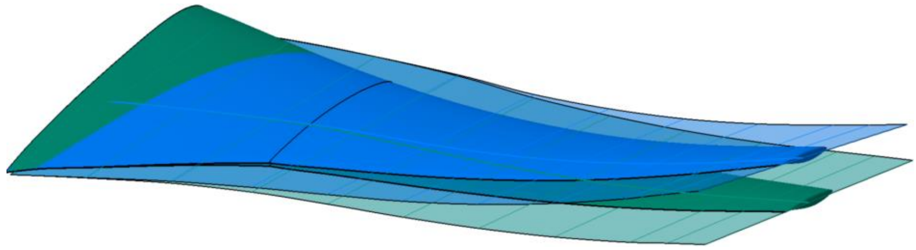

Figure 10 - Original and deformed wing and their transformation surfaces

Control of the deformation

In the comparison of original and deformed geometry, the following values were determined for the worst case of the wind tunnel test - the largest angle of attack at the larger Reynolds number:

Geometric Feature	Original	Deformed	Difference	Absolute Δ in Wind Tunnel Scale
Length of the center curve	30564.346mm	30564.340mm	0.00002%	-0.16 μm
Area of the lower wing	171.967m²	171.864m²	0.05990%	-0.75 cm²
Wing chord at 80% span	4090.474mm	4086.62mm	0.09422%	-29.14 μm
Airfoil thickness at 80% span	381.842mm	381.699mm	0.03745%	-11.75 μm

Table 2 - Overview of the geometric deviation

Input data for mesh deformation

Based on the newly obtained surfaces, a mesh redefinition can be performed as shown in branch (b) on Fig. 2. To perform the mesh deformation (a), the transformation vectors are needed, each of which describes the translation between the initial position and the deformed wing. Again, the quality of the result depends on that of the input data: A generation by e.g. sections parallel to symmetry plane would give imprecise results due to the bending of the wing, because different spanwise positions would be compared.

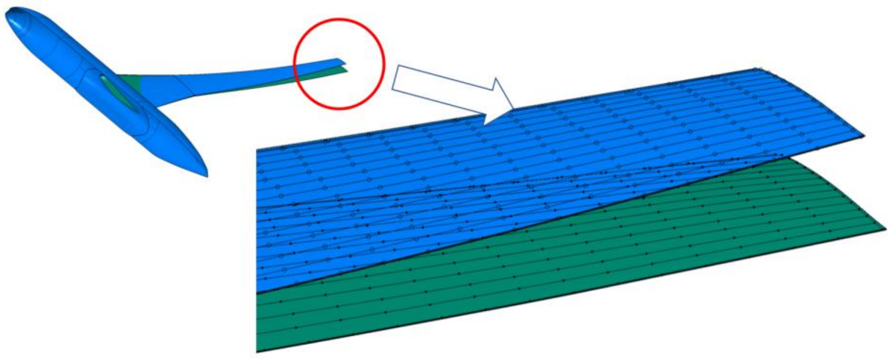

Figure 11 - Curves and points to calculate the transformation vectors

To achieve an average point spacing of about 500mm, 15 points of equal spacing were distributed on the wing airfoil of the kink for both wing versions on the upper and lower side. By these, spanwise isoparametric curves are generated. On each of these curves, equidistant points with a distance of about 500mm were distributed, depending on the curve length between 60 and 67 points. In total, 1876 transformation vectors were generated.

4. Verification

A verification has been performed in order to evaluate the overall quality of the deformed aerodynamic surfaces generated by the presented method and their suitability for CFD mesh generation and transonic flow simulations. In particular the influence of

- the differences found in wing reference area, chord length and profile thickness between the baseline and the deformed wing geometry, Table 2, and
- the deviations in wing twist between the current deformed geometries and the geometries used in DPW-6, applying the deformation method described in [1][1].

on overall aerodynamic parameters, like lift and drag coefficients, and the wing's static pressure distribution was assessed.

Two unstructured CFD meshes were generated on the flight shape for q/E = 0.3260 and α = 4.00°, one using the geometry from CATIA's "Wrap Surface" function method described in Section 3 of this paper, and a second one based on the geometry obtained from the CADfix (ITI TranscenData) "Geometry Deformation" feature (1), which was used for DPW-6. To reduce any CFD mesh influence on the numerical results the grids were generated to be as similar as possible with unstructured grids.

	DPW-6 Geometry	**DPW-7 Geometry**	**Δ / [%]**
Wing Surface Points	614,308	612,347	0.3197
Wing Surface Elements	1,228,004	1,224,090	0.3192
Volume Points	23,284,916	23,207,677	0.3323
Boundary Layer Prisms	43,686,195	43,542,485	0.3295
Farfield Tetrahedra	6,530,459	6,504,463	0.3989

Table 3 - Comparison of CFD grids

Transonic RANS flow simulations were performed at Ma = 0.85 and Re = 5.0×10^6 (based on wind tunnel model reference chord length $c_{ref.}$ = 189.14mm/7.447in) and aerodynamic coefficients and static pressure distributions obtained on the two geometries were compared. The differences of overall aerodynamic coefficients between the CFD analyses on the DPW-6 and DPW-7 geometries were found to be sufficiently small (Table 3).

Coefficient	**Δ**
C_L	0.001354
C_D	0.000435
C_M	-0.004236

Table 4 - Difference of overall aerodynamic coefficients between DPW-6 and DPW-7 geometries

To gain a more detailed insight into the flow over the two geometries, static pressure distributions were extracted from the wing surfaces in nine spanwise sections (Table 4). The agreement of pressure distributions on both geometries (Figure 12), was found to be very good, with minor deviations occurring in shock location and rooftop pressure levels for some sections.

[1] The largest delta in twist was found to be $\Delta\varepsilon \approx 0.07$deg at wing tip ($\eta$ = 0.98).

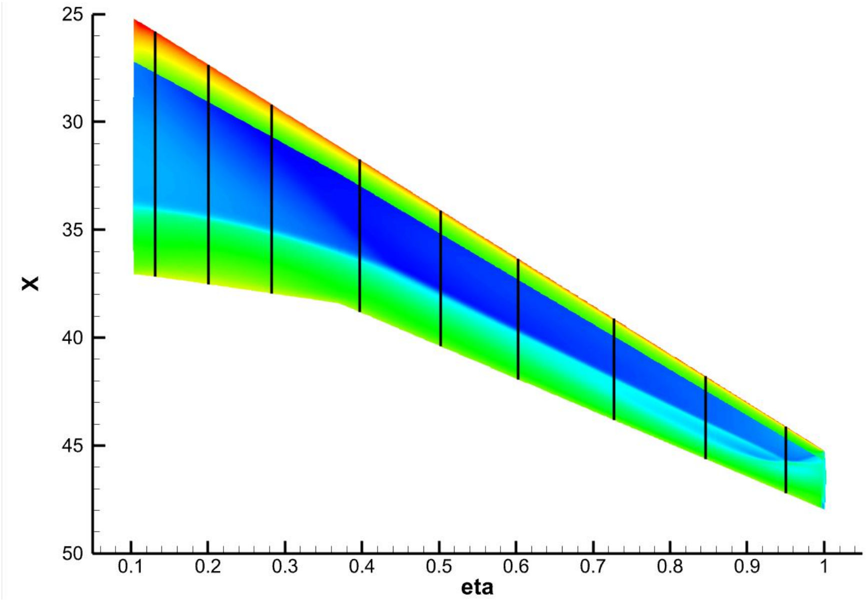

Figure 12 - Spanwise sections y=const. for static pressure analyses

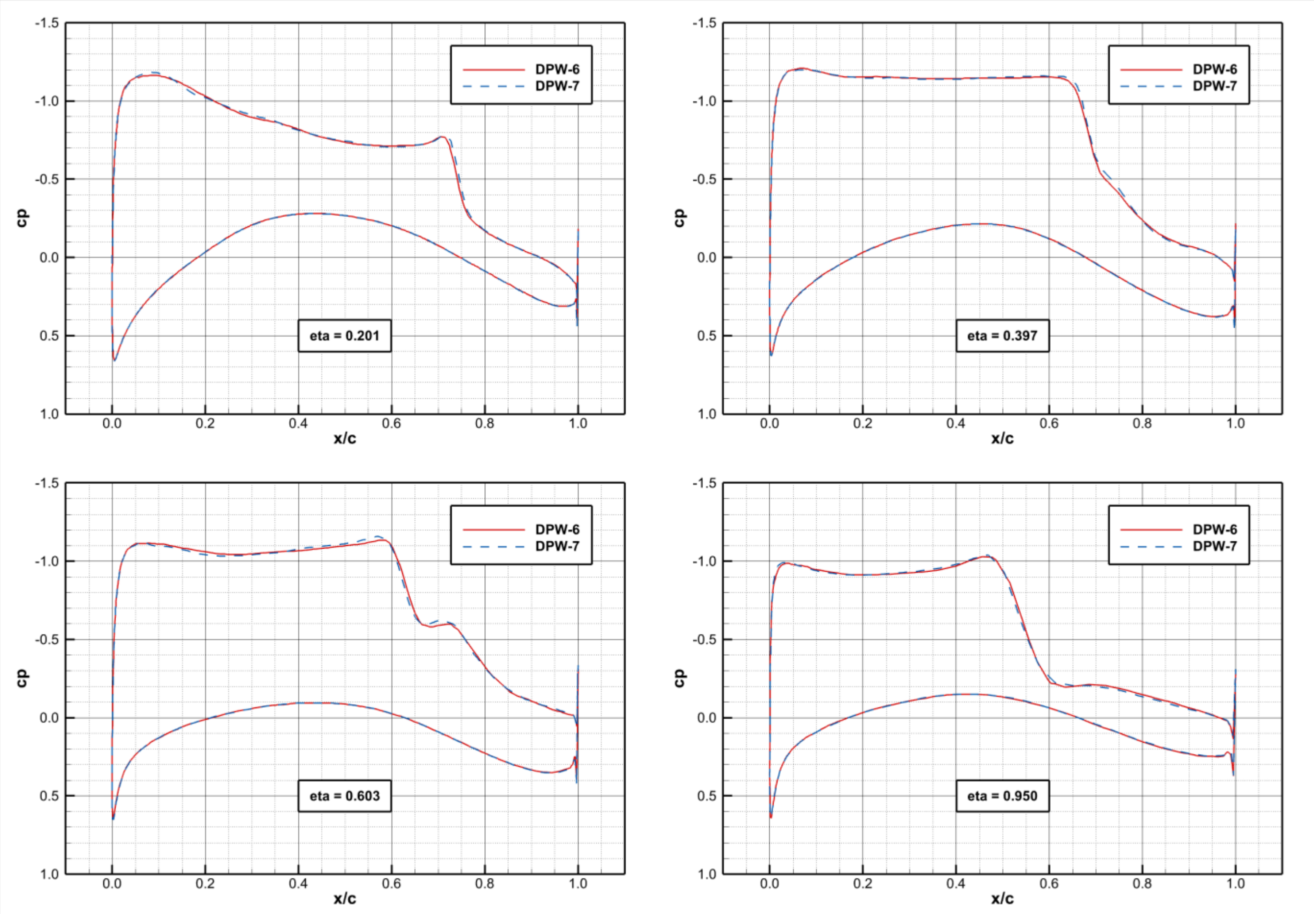

Figure 13 - Comparison of selected static pressure distributions obtained on DPW-6 and DPW-7 geometries

The verification results show that the observed deviations of wing planform geometry and profiles between the two deformed CAD geometries do not have any adverse effects on the numerical flow simulations in the transonic regime. The simulation therefore prove that the method for deforming CAD geometry representations is applicable in the context of CFD without any constraints.

Discussion

In the transfer of the vertical deflection, straight sections were assumed between the sections due to the spherical surfaces. Thus, the curved original mean curve is approximated by a polygonal curve. The real center curve of the deformed wing will form a curved shape, resulting in a deviation in the applied method. However, since the exact shape of the real center curve is unknown, the deviation to be assumed was accepted as negligible. The small deviation of the achieved values in span and wing area confirms this assumption. The mesh fineness of about 500mm in the generation of the transformation vectors was not further varied. The achieved deviation during validation shows that this value is in plausible order of magnitude. A more detailed investigation of the influence of this mesh fineness would be a rational extension.

5. Summary and outlook

It has been shown that the CAD function "Wrap Surface" provided by the CAD system CATIA can be applied in the context of aeroelastic deformation. This allows an improved correlation between CFD results and wind tunnel data without the previously used method of having to perform parallel aeroelastic analyses, which would require coupling with a structural model. Especially the integration in form of a function of the used CAD system without the need of secondary software tools allows a continuous process chain, where the deformation is only an intermediate step of the parametric design. It is advantageous - especially for multidisciplinary investigations - that at any time the CFD geometry is available as a three-dimensional surface model without having to perform a back transformation from the deformed meshes. The method of mesh deformation is subject to limitations as the complexity of the geometry under investigation increases. Modeling this step in terms of CAD deformation provides the opportunity to use the deformed geometry for follow-on structures that remain undeformed. An example would be the engine and pylon, which require circular elements.

6. Contact Author Email Address

The following email addresses are available for contacting the authors: patrick.wegener@dlr.de, stefan.keye@dlr.de.

Acknowledgements

ETW deformation data were kindly provided by Dr.-Ing. Thorsten Lutz, Institut für Aerodynamik und Gasdynamik, Universität Stuttgart. Interpolated deformation data was kindly provided by E. Tinoco, member DPW Organizing Committee.

Copyright Statement

References

[1] Keye S, Gammon M R. Development of Deformed CAD Geometries of NASA's Common Research Model for the Sixth AIAA CFD Drag Prediction Workshop, *34th AIAA Applied Aerodynamics Conference*, 2016.

[2] Boyet G. ESWIRP: European Strategic Wind tunnels Improved Research Potential program overview, *CEAS Aeronautical Journal,* 9. Jg., Nr. 2, 2019.

[3] 6th AIAA CFD Drag Prediction Workshop [online database], *AIAA*, Reston, VA, 2015, http://aiaa-dpw.larc.nasa.gov/ [retrieved 05 July 2017].

[4] Vassberg J, DeHaan M A, Rivers M S, Wahls R A. Development of a Common Research Model, *AIAA*, 2008.

[5] Keye S, Rudnik R. Validation and Assessment of Turbulence Model Impact for Fluid-Structure Coupled Computations of the NASA CRM. *CEAS Aeronautical Journal*, 2015.

[6] Ronzheimer A. CAD in aerodynamic aircraft design. *DGLRK*, 2017

[7] Common Research Model [online database], *NASA*, 2015, http://commonresearchmodel.larc.nasa.gov/ [retrieved 24 May 2022].